

# Substituent Effects on Two-Center Three-Electron Bonds and Hydrogen Bonds Involving Unsaturated Organic Functional Groups and an Ammonia Radical Cation—The Resonance Contribution

Stéphane Humbel,<sup>\*,[a]</sup> Norbert Hoffmann,<sup>[b]</sup> Isabelle Côte,<sup>[a]</sup> and James Bouquant<sup>[a]</sup>

*Dedicated to the memory of Professor Josselin Chucho*

**Abstract:** A theoretical investigation of the substituent effects on the two-center, three-electron ( $2c-3e$ ) bond involved between unsaturated functional groups and an amine nitrogen is presented. The competitive hydrogen-bonded complexes are also studied. In both cases, the bond energies are found to be in the range of 20–30 kcal mol<sup>-1</sup>. The variation of these energies is discussed with respect to the electron-donating effect of

the substituents, as well as with respect to the  $\pi$ -bonded atom of the organic functional group (O, S, NH). For the  $2c-3e$  bonds, the results are discussed on the basis of the differences of the ionization potential ( $\Delta IP$ ) of the separated frag-

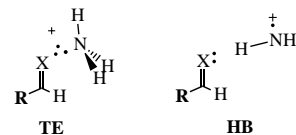
**Keywords:** ab initio calculations • hydrogen bonds • ion-molecule complex • resonance model

ments and can be rationalized through the valence bond theory. For the hydrogen bonds, the substituent influence is discussed by using the differences of the proton affinities ( $\Delta PA$ ) of the substrates. The resonating nature of the hydrogen bond in these cationic systems is investigated and is found to account for most of the binding energy. Marcus theory is compared with the proposed resonating model.

## Introduction

When they involve saturated organic functional groups, two-center, three-electron ( $2c-3e$ ) bond complexes are frequent in both experimental and theoretical studies.<sup>[1–4]</sup> These bonds are mainly involved in charged symmetrical systems, when both hemibonded partners possess a similar ionization potential (IP). This point is well explained by the resonating nature of the hemibonded species<sup>[5]</sup> and has been demonstrated elsewhere.<sup>[6]</sup> Let us just remind here that the bond strengths are shown to be larger for a small difference in the ionization potentials of the partners.<sup>[1b]</sup> They are thus favored in symmetrical systems, but one may consider the cases of unsymmetrical systems in which both partners possess similar, but not equal, IPs. Those are expected to form a  $2c-3e$  bond. Curiously a relatively small number of unsymmetrical  $2c-3e$  bonded systems are discussed in the literature.<sup>[7]</sup>

In the class of unsymmetrical  $2c-3e$  bonded systems, we have recently studied the case of complexes that contain unsubstituted unsaturated functions (like carbonyl, thiocarbonyl, or imine) and the radical cation of ammonia ( $NH_3^{\cdot+}$ ).<sup>[8]</sup> We showed that these unsaturated compounds might form stable  $2c-3e$  bonded complexes with the radical cation of ammonia despite the fact that the  $2c-3e$  bonds were unsymmetrical. These unsaturated functional groups are expected to possess a great sensitivity to the electronic effects of the substituents, especially when  $\pi$  donors are involved. Here we aim to study the substituent effects on the  $2c-3e$  bonded species that might be formed between substituted, unsaturated organic functional groups and the radical cation of ammonia (**TE**).<sup>[9]</sup>



Our compounds might also form a hydrogen-bonded complex (**HB**). The hydrogen bonds in these radical cations can be classified as “short–strong” (SSHB) or “low-barrier” hydrogen bonds (LBHB).<sup>[10]</sup> The later term indicates the fact that the barrier of the proton transfer from the nitrogen atom onto the X atom is low in energy. Whether or not a system possesses such a barrier has been the subject of many publications in the past years and is still an important problem. Scheiner, for instance, performed detailed studies on this problem by calculating the appearance of a barrier

[a] Dr. S. Humbel, I. Côte, Prof. J. Bouquant  
Groupe de Modélisation et Réactivité Chimique, UMR 6519/CNRS  
Université de Reims-Champagne-Ardenne, UFR Sciences BP 1039  
51687 REIMS Cedex 2 (France)  
Fax: (+33)326-91-31-66  
E-mail: stephane.humbel@univ-reims.fr

[b] Dr. N. Hoffmann  
Groupe de Photochimie, UMR 6519/CNRS  
Université de Reims-Champagne-Ardenne, UFR Sciences BP 1039,  
51687 REIMS Cedex 2 (France)

Supporting information for this article is available on the WWW under <http://www.wiley-vch.de/home/chemistry/> or from the author. The complete geometries of each species ( $x, y, z$  coordinates) can be found in the supporting information together with their absolute energies.

when varying the distance between the heavy atoms involved in the bond.<sup>[11]</sup> In this paper we will not focus on the barrier height, which is small and can appear or disappear depending on the level of calculation.<sup>[12]</sup> Rather we wish to concentrate on the resonating nature of the bonds.

In the following we shall thus answer these questions:

- 1) What is the range of energies of both the 2c–3e and the hydrogen bonds?
- 2) How do the substituents modify the 2c–3e bond strength?
- 3) How do they modify the hydrogen bond strength?
- 4) How does the resonance contribute to the hydrogen bond in those cationic systems?

## Computational Details

The calculations were carried out by using the Gaussian 94 package.<sup>[13]</sup> The optimizations were all done at the unrestricted MP2/6-31G(d) level (frozen core) and the stationary points were characterized by mean of analytical second derivatives. Cartesian d orbitals were used (6D) at this stage. This level of calculation usually gives satisfactory results for both hydrogen bonds and 2c–3e bonded complexes. However, we intend to use calculated ionization potentials and proton affinities of each fragment involved. These quantities usually require large basis sets and a high level of calculation to take into account the modification of the electronic correlation. The energy calculations were thus performed by using the substantially larger basis set from Dunning<sup>[14]</sup> (aug-cc-pvdz)<sup>[15]</sup> and at a significantly higher level of calculation (MP4). However, owing to a substantial spin contamination in some cases ( $\langle S^2 \rangle$  up to 0.89), we shall only use in the following the projected MP3 values (noted PMP3). The spin contamination after projection was always found to be very small ( $\langle S^2 \rangle$  up to 0.76). This calculation level, PMP3/aug-cc-pvdz, was found to predict correctly the coupled cluster results (CCSD(T)) in our previous study.<sup>[8]</sup> Similar results about the PMP3 quality relative to the CCSD(T) level have also been obtained by using the IMOMO-ONIOM<sup>[16]</sup> method in the case of carbonyl derivatives ( $X = O$ ).<sup>[17]</sup>

## Results

The potential energy surface (PES) of interest is depicted in Figure 1. The label  $\mathbf{x}$  stands for carbonyls ( $\mathbf{x} = \mathbf{1}$ ), thiocarbon-

**Abstract in French:** *Nous présentons ici une étude théorique des effets de substituants sur des liaisons à deux centres et trois électrons (2c–3e) mises en jeu entre une fonction organique insaturée et l'atome d'azote d'amines. La liaison hydrogène qui est compétitive avec cette interaction est aussi étudiée. Les énergies de liaisons sont trouvées comparables (20–30 kcal mol<sup>-1</sup>). Les variations de ces énergies de liaisons sont analysées en fonction de l'effet donneur des substituants et de l'hétéro-atome des différentes fonctions insaturées (O, S, NH). Pour les liaisons de type 2c–3e, cette discussion s'appuie sur la différence de potentiels d'ionisation et trouve sa base dans la théorie de la liaison de valence (Valence Bond). Les liaisons hydrogène sont commentées en fonction de la variation de l'affinité protonique des partenaires. La nature résonante de ces liaisons hydrogènes dans des cations est étudiée et trouvée comme étant la cause majoritaire de la stabilisation par liaison hydrogène. La théorie de Marcus est comparée au modèle résonant que nous proposons.*

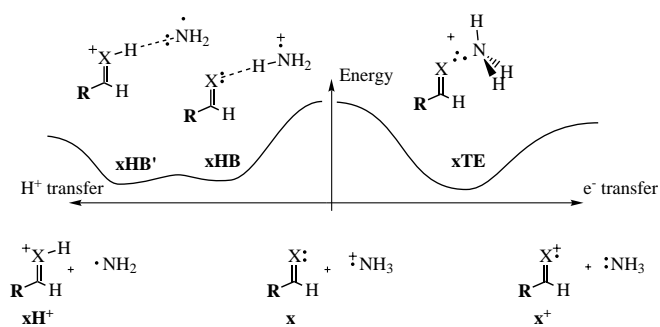


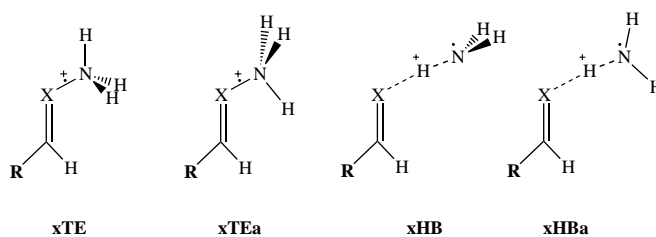
Figure 1. Qualitative potential energy surface of interest,  $X = O, S, NH$  and  $R = H, CH_3, NH_2$ .

yls ( $\mathbf{x} = \mathbf{2}$ ), and imines ( $\mathbf{x} = \mathbf{3}$ ), while  $\mathbf{R}$  stands for the substituent ( $H, CH_3, NH_2$ ). Starting from  $\mathbf{x} + NH_3^{*+}$ , in the middle, we will first study the single electron transfer (SET) reaction (right-hand side). This path leads to the radical cation of the unsaturated species ( $\mathbf{x}^+$ ) and the closed-shell ammonia. It goes through the local minimum of the 2c–3e bonded intermediate  $\mathbf{xTE}$ .

As mentioned in the introduction, the investigated species might also form a hydrogen bonded complex, which is on the way of the proton transfer reaction depicted on the left-hand side of Figure 1. This path might go through a hydrogen bonded species  $\mathbf{xHB}$  (involving  $\mathbf{x}$  and  $NH_3^{*+}$ ), then through a second type of hydrogen bond denoted  $\mathbf{xHB}'$  (involving  $\mathbf{xH}^+$  and  $\cdot NH_2$ ), and finally leads to the separated protonated species ( $\mathbf{xH}^+$ ) and the  $\cdot NH_2$   $\pi$  radical. The barrier between  $\mathbf{xHB}$  and  $\mathbf{xHB}'$  was found to be extremely low in energy and most frequently, we obtained only one type of hydrogen bond complex,  $\mathbf{xHB}$  or  $\mathbf{xHB}'$ , on a very shallow potential energy surface (PES). The barrier for the proton transfer inside radical-cation complexes is indeed frequently found to be either extremely low or non existent.<sup>[11, 18]</sup>

Both  $\sigma$  ( $R = CH_3$ ) and  $\pi$  ( $R = NH_2$ ) electron-donating effects were studied and compared with the corresponding unsubstituted systems ( $R = H$ ). It is noteworthy that the  $\pi$ -donating effect of the  $NH_2$  substituent contributes only moderately to the stabilization of the 2c–3e bond as well as to the hydrogen bond, since these bonds are of  $\sigma$  type (located at the lone pair of the organic functional groups).

**Geometry optimizations:** The geometry optimizations of the complexes  $\mathbf{xTE}$  and  $\mathbf{xHB}$  (or  $\mathbf{xHB}'$ ) were carried out in  $C_s$  symmetry and checked as minima by means of frequency analysis.<sup>[19]</sup> All our calculations deal with an approach of the ammonia from the *trans* side of the substituent. The other approach (*cis* side) was indeed found to lead to species slightly higher in energy. For the 2c–3e bonded complexes we always



present here the compound of type **xTE** rather than the rotated compound **xTEa**. In fact, a nearly free rotation around the X–N axis was observed. For the hydrogen bonded complexes, two kinds of structures were investigated, the twisted **xHB** and the planar **xHBa**. Only in the  $\text{H}_2\text{C}=\text{O}$  case was the **xHBa** structure found to be energetically favored. All the other cases were twisted (**xHB**). However, the energy difference is extremely small.

Whether the hydrogen bonded complexes should be expected as **HB**-like or as **HB'**-like (Figure 1 left-hand side) is indicated by the sign of the difference of proton affinity (vide infra).

**Fragments:** The fragments of the PES are of a special interest as they provide the starting point for both ionization potentials (IP) and proton affinities (PA) of the substrates. The important geometrical parameters of the MP2/6-31G(d) optimized unsaturated neutral fragments are displayed in Figure 2. Except for the formamide ( $\text{X}=\text{O}$ ,  $\text{R}=\text{NH}_2$ ) and the formamidine ( $\text{X}=\text{NH}$ ,  $\text{R}=\text{NH}_2$ ) whose nitrogen is found to

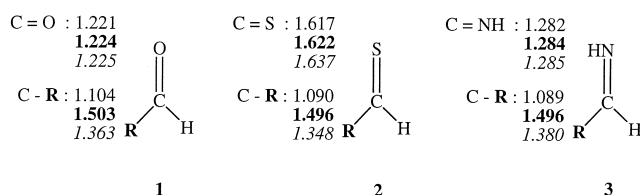


Figure 2. Main geometrical parameters (bond lengths in Å) of the neutral unsaturated fragments as optimized at the MP2/6-31G(d) level. **R** = H (plain),  $\text{CH}_3$  (bold), and  $\text{NH}_2$  (italic).

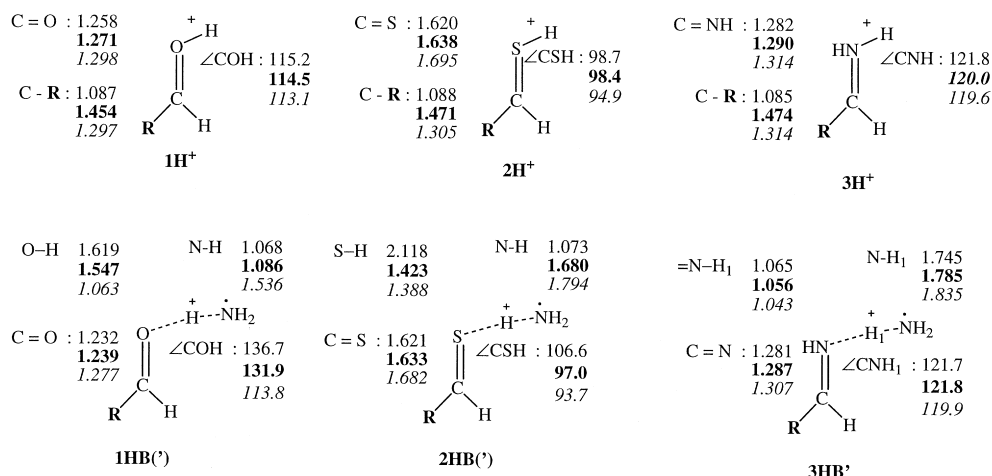


Figure 4. Main geometrical parameters (bond lengths in Å, bond angles in °) of the proton transfer fragments (**xH<sup>+</sup>**) and of the hydrogen bonded species as optimized at the MP2/6-31G(d) level. These might be either **HB**- or **HB'**-like, depending on the sign of  $\Delta\text{PA}$  (see text). **R** = H (plain),  $\text{CH}_3$  (bold), and  $\text{NH}_2$  (italic).

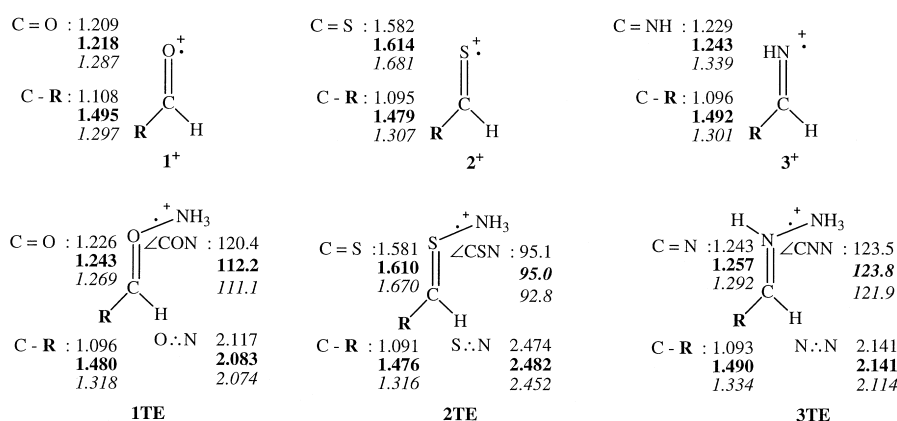


Figure 3. Main geometrical parameters (bond lengths in Å, bond angles in °) of **x<sup>+</sup>** and **xTE** as optimized at the MP2/6-31G(d) level. **R** = H (plain),  $\text{CH}_3$  (bold), and  $\text{NH}_3$  (italic).

be pyramidalized at this level of calculation and thus adopt a  $C_1$  symmetry, all these fragments bear a  $C_s$  symmetry.

**2c-3e:** The dissociation fragments of the 2c-3e bonded species **xTE** might be either the starting materials (**x** +  $\text{NH}_3^+$ ) or the SET products (**x<sup>+</sup>** +  $\text{NH}_3$ ). Figure 3 displays the main geometrical parameters of the **x<sup>+</sup>** fragments and of the 2c-3e bonded complexes **xTE**. Except for the radical cation of the formamidine fragment, which has an out of plane hydrogen and thus adopts a  $C_1$  symmetry, all these species bear a  $C_s$  symmetry. The bond lengths for these complexes are rather large, since such 2c-3e bonds are most stabilized for a low overlap ( $S = 1/3$ ) between the fragments.<sup>[1a, 5]</sup>

**Hydrogen bonds:** The dissociation fragments of the hydrogen bonds might be either the starting materials (**x** +  $\text{NH}_3^+$ ) or the proton transfer products (**xH<sup>+</sup>** +  $\text{NH}_2$ ) (see Figure 1 left-hand side). Figure 4 displays the main geometrical parameters of the **xH<sup>+</sup>** fragments and of the hydrogen bonded complexes **xHB** or **xHB'**. All the species possess a  $C_s$  symmetry. The nature of the preferred hydrogen bond is indicated by the sign of  $\Delta\text{PA}$ , that is, the difference in proton affinities as obtained

from Equation (1): **HB**-like structures for  $\Delta\text{PA} > 0$  and **HB'** when  $\Delta\text{PA} < 0$ . The proton affinities are displayed and discussed later.

$$\Delta\text{PA} = \text{PA}(\text{x}) - \text{PA}(\cdot\text{NH}_2) \quad (1)$$

Positive  $\Delta\text{PA}$  are encountered in three systems that are carbonyls with  $\text{R} = \text{H}$  or  $\text{CH}_3$  and thiocarbonyl when  $\text{R} = \text{H}$ . For the other systems **HB'**-like hydrogen bonds are expected to be lower in energy than **HB**-like hydrogen bonds ( $\Delta\text{PA} < 0$ ). In some rare cases (for the smallest  $\Delta\text{PA}$ s) we found both **HB**- and **HB'**-like structures. Only the preferred structures (according to the sign of  $\Delta\text{PA}$ ) are presented in Figure 4.

**Calculated potential energy surfaces:** Figure 5 displays the potential energy surfaces calculated in this work. Here, we would like to comment on the main trends when comparing 2c–3e and hydrogen binding for these systems.

It is shown that in carbonyl cases (**1**), the hydrogen bonded species are about  $7 \text{ kcal mol}^{-1}$  more stable than the corresponding 2c–3e bonded species. For the thiocarbonyl species (**2**) the order of stability is reversed and the hydrogen bonded complexes are more than  $20 \text{ kcal mol}^{-1}$  higher in energy than the corresponding 2c–3e bonded species. This is not very

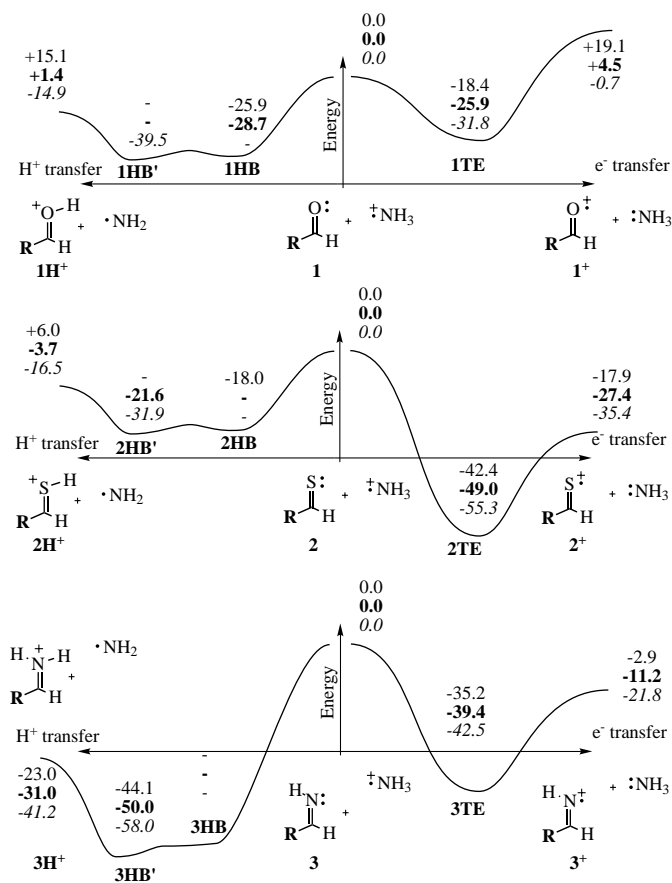


Figure 5. The potential energy surfaces ( $\text{kcal mol}^{-1}$ ) as calculated at the PMP3/aug-cc-pvdz//MP2/6–31G(d) level. The substituent on the organic function is noted as follows:  $\text{R} = \text{H}$  (plain),  $\text{CH}_3$  (bold), and  $\text{NH}_2$  (italic). The different functions are presented in the different parts: **1** for carbonyl (top), **2** for thiocarbonyls (middle), and **3** for imines (bottom).

surprising taking into account the usual reluctance of sulfurs to form an hydrogen bond. Finally, in the case of the imines (**3**), the hydrogen bonded species are about  $10 \text{ kcal mol}^{-1}$  more stable than the 2c–3e bonded species. This result is more surprising because the homonuclear N–N bond was expected to be among the strongest 2c–3e interactions. However, the hydrogen bonded species are of the type **HB'**, which means that a proton has already transferred onto the nitrogen of the imine. The hydrogen bonded complex therefore involves an iminium ion and the  $\cdot\text{NH}_2$  radical moiety. Those iminiums are known to be very stable. Note that the dissociative fragments of the  $\text{NH}_2$  substituted imine case (amidinium) are especially stable ( $-41.2 \text{ kcal mol}^{-1}$ ), nearly as stable as the 2c–3e bonded complex. This stability is well explained through the symmetrical charge delocalization which can occur in the amidinium and drives down the PES toward stable hydrogen bonded complexes.

## Discussion

It is noteworthy that in the carbonyl cases the substituent effect *increases* the 2c–3e binding energy (as calculated with respect to the lowest dissociative fragments) from  $18.4$  ( $\text{R} = \text{H}$ ) up to  $31.1 \text{ kcal mol}^{-1}$  ( $\text{R} = \text{NH}_2$ ), while this effect *decreases* it in the imine cases (from  $32.2$  down to  $20.7 \text{ kcal mol}^{-1}$ ).<sup>[20]</sup> The same electron-donating effect leads to an opposite behavior depending on the nature of the X atom. The substituent effects can be analyzed in detail by using the resonating nature of the bonds. The 2c–3e binding is well known to be a purely resonance phenomena, and we will see how this aspect can be used to understand the substituent effects on the binding energies.

**Resonance:** In a dissymmetric 2c–3e bonded system, say  $[\text{A}\cdot\text{B}]^+$  for instance, the 2c–3e bond is depicted as a resonance between the valence bond structures  $\text{AB}^+$  and  $^+\text{AB}$ . As usual, the resonance would be larger if the difference in energy between the resonating structures is small.



In a previous publication we detailed how the resonance can be depicted in 2c–3e bonds using these two resonating structures.<sup>[6]</sup> The difference in energy between the structures  $\text{AB}^+$  and  $^+\text{AB}$  is an important factor and we approximated it as the energy difference between the ionization potentials of A and B ( $|\Delta\text{IP}|$ ). Going from  $\text{AB}^+$  to  $^+\text{AB}$  requires the removal of one electron from the lone pair of the fragment A in  $\text{AB}^+$  and to pass it to the B<sup>+</sup> fragment.

Another important factor is the coupling constant between the resonating structures; this was approximated to  $-(D_{\text{AA}} + D_{\text{BB}})/2$  when both partners are close in energy, where  $D_{\text{AA}}$  and  $D_{\text{BB}}$  are the binding energies of the symmetrical systems  $\text{A}\cdot\text{A}$  and  $\text{B}\cdot\text{B}$ , respectively. This simply means that if  $|\Delta\text{IP}|=0$ , the binding energy of the  $\text{A}\cdot\text{B}$  system would be in between those of  $\text{A}\cdot\text{A}$  and  $\text{B}\cdot\text{B}$ .

Solving the resonating system for  $|\Delta\text{IP}| \neq 0$  led to Equation (2) below, which was transformed in Equation (3) when  $\Delta\text{IP}$  is small before  $(D_{\text{AA}} + D_{\text{BB}})/2$ . Equation (3) shows the exponential dependency of  $D_{\text{AB}}$  toward  $|\Delta\text{IP}|$  formerly mentioned by Clark.<sup>[1b]</sup>

$$D_{\text{AB}} = -(|\Delta\text{IP}| - \sqrt{|\Delta\text{IP}|^2 + (D_{\text{AA}} + D_{\text{BB}})^2})/2 \quad (2)$$

$$D_{\text{AB}} \approx [(D_{\text{AA}} + D_{\text{BB}})/2] \exp(-|\Delta\text{IP}|/2\sqrt{D_{\text{AA}}D_{\text{BB}}}) \quad (3)$$

In the following discussion we will keep in mind the  $|\Delta\text{IP}|$  dependency to discuss the substituent effects on the 2c–3e bond strength. Equation (2) will also be adapted to the hydrogen binding for numerical tests on the resonating nature of the cationic hydrogen bond.

**2c–3e bond strength analysis:** The relevant calculated IPs are displayed in Table 1. As expected, they all decrease as the substituent-donating effect increases (H, CH<sub>3</sub>, NH<sub>2</sub>), stabilizing the cationic species more than the neutral one. Moreover, we are concerned with the *difference* between the ionization potentials. It is found here that when **R** = H or CH<sub>3</sub>, the carbonyl compound has a higher IP than the one of the NH<sub>3</sub>

Table 1. Ionization potentials [kcal mol<sup>-1</sup>] of the fragments as calculated at the PMP3/aug-cc-pvdz level.<sup>[a,b]</sup>

Systems	H <sup>[c]</sup>	<b>R</b>	
		CH <sub>3</sub>	NH <sub>2</sub>
IP(1)	247.3	232.7	227.5
IP(2)	210.3	200.9	192.9
IP(3)	225.4	217.0	206.5

[a] As calculated at the same level, the IP of NH<sub>3</sub> accounts for 228.2 kcal mol<sup>-1</sup>. [b] **1** stands for the carbonyls, **2** for the thiocarbonyls, and **3** for the imines. [c] From ref. [8].

moiety. The aforementioned single electron transfer (SET) path shall thus be endothermic in these two cases. In contrast, all the other species (amide, thiocarbonyls, and imines) possess lower IPs than that of ammonia, and the SET path is thus found to be exothermic in these cases.

It is also noteworthy that in some cases the IPs of the organic substrates are very close to the IP of NH<sub>3</sub>, particularly for the formamide (**X** = O, **R** = NH<sub>2</sub>) and for the unsubstituted imine (**X** = NH, **R** = H). According to the resonance model, these are the cases we expect to form the strongest 2c–3e bonds.

As mentioned earlier, the bond strength has to be calculated with respect to the lower dissociative fragments, which are indicated by the sign of  $\Delta\text{IP}$  when calculated with Equation (4).

$$\Delta\text{IP} = \text{IP}(\mathbf{x}) - \text{IP}(\text{NH}_3) \quad (4)$$

A positive  $\Delta\text{IP}$  reveals that the starting materials (Figure 1) are the lower dissociative fragments, while a negative  $\Delta\text{IP}$  points out that the SET products ( $\mathbf{x}^+ + \text{NH}_3$ ) are the lower dissociative fragments. Table 2 indicates the relative energies that are relevant for the following discussion.

Table 2.  $\Delta\text{IP}$  values<sup>[a]</sup> relative to the  $\mathbf{x} + \text{NH}_3^+$  starting materials (plain) [Eq. (4)], and 2c–3e bond strength (italic) as calculated using the lowest dissociative fragments of the 2c–3e bond.

Species	H <sup>[b]</sup>	<b>R</b>	
		CH <sub>3</sub>	NH <sub>2</sub>
<b>1</b> + NH <sub>3</sub> <sup>+</sup>	0.0	0.0	0.0
<b>1</b> <sup>+</sup> + NH <sub>3</sub>	( $\Delta\text{IP}$ )	19.1	4.5
<b>1TE</b>	( $D_0$ )	<i>18.4</i>	<i>25.9</i>
<b>2</b> + NH <sub>3</sub> <sup>+</sup>	0.0	0.0	0.0
<b>2</b> <sup>+</sup> + NH <sub>3</sub>	( $\Delta\text{IP}$ )	–17.9	–27.4
<b>2TE</b>	( $D_0$ )	<i>24.5</i>	<i>21.6</i>
<b>3</b> + NH <sub>3</sub> <sup>+</sup>	0.0	0.0	0.0
<b>3</b> <sup>+</sup> + NH <sub>3</sub>	( $\Delta\text{IP}$ )	–2.9	–11.2
<b>3TE</b>	( $D_0$ )	<i>32.2</i>	<i>28.2</i>

[a] In kcal mol<sup>-1</sup> at the PMP3/aug-cc-pvdz//MP2/6–31G(d) level of calculation. [b] From ref. [8].

In the carbonyl cases in which fragments **1**<sup>+</sup> and NH<sub>3</sub> are higher in energy than **1** + NH<sub>3</sub><sup>+</sup> (**R** = H or CH<sub>3</sub>), the electron-donating effect, by lowering **1**<sup>+</sup> + NH<sub>3</sub> energy, diminishes the  $\Delta\text{IP}$  value, and thus increases the 2c–3e bond strength. The largest 2c–3e bond strength in this series is encountered in the formamide case (**X** = O, **R** = NH<sub>2</sub>) with a small negative  $\Delta\text{IP}$  (–0.7 kcal mol<sup>-1</sup>). As the *absolute value* of  $\Delta\text{IP}$  is continuously decreasing in this series, we find a continuous increase of the 2c–3e bond strength.

As we shall see in the following, one should certainly not consider as a rule that a stronger electron-donating effect should lead to a stronger 2c–3e bond as is the case above. The thiocarbonyl and imine series illustrate this point. As indicated by the negative values of  $\Delta\text{IP}$ , the lower dissociative fragments of the unsubstituted 2c–3e complex are the cationic species  $\mathbf{x}^+$  and the neutral ammonia NH<sub>3</sub>. Increasing the electron-donating ability of the substituent leads to a further stabilization of the fragments  $\mathbf{x}^+ + \text{NH}_3$  with respect to  $\mathbf{x} + \text{NH}_3^+$ . As a consequence, the  $\Delta\text{IP}$  *absolute value* increases and thus the 2c–3e binding energy diminishes.

This simple analysis not only explains an opposite behavior of the 2c–3e bond strength toward substituent-donating effect, that is, an *increase* of the 2c–3e bond strength in the carbonyl case, while a *decrease* is found in the other cases. It also permits us to predict how the 2c–3e bond strength would vary beyond our examples: The complex between the carbonyl species and the radical cation of ammonia was found to exhibit a larger 2c–3e bond energy as the substituent-donating effect increases. Lets consider now, for instance, a further increase in the electron-donating effect of **R** = NH<sub>2</sub> in the formamide (as it would be the case in *N,N*-dimethylformamide, **R** = N(CH<sub>3</sub>)<sub>2</sub>). One should expect  $\Delta\text{IP}$  to decrease significantly in value (more negative), but, and more importantly for our matter, to *increase in absolute value*. It is noteworthy to mention how the same electron-donating effect, which was contributing to increase the 2c–3e bond strength up to this point, would now contribute to decrease it. Figure 6 qualitatively illustrates the relationship between the electron-donating effect and the bond energy.

Moreover, this whole study not only provides an efficient tuning strategy to strengthen or circumvent the 2c–3e interaction by the use of electron-donating or -withdrawing substituents on both reaction partners. Its spirit might also be

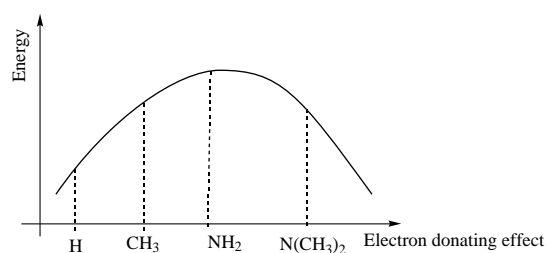


Figure 6. Qualitative modification of the 2c–3e binding energy when increasing the electron-donating effect of the substituent on the carbonyl.

applied to the hydrogen bond strength as we shall see in the following.

While the ionization potential (IP) of the unsaturated moiety decreased as the electron-donating effect of **R** increased, the proton affinities (PA) increase as the electron-donating effect of **R** increased.

**Hydrogen bond strength:** The hydrogen bond strength can easily be related to the basicity (proton affinity, Table 3) of the organic species. For **HB**-like systems (Figure 4 and 5), electron-donating substituents increase the basicity on the heteroatom of the unsaturated organic functional group. It is thus well understood why the hydrogen bond strength increases (Table 4) when increasing the electron-donating effect of the substituent. For **HB'**-like hydrogen bonds ( $\Delta\text{PA} < 0$ ), the bond strength should be related to the acidity of the hydrogen on the **X** atom of the protonated organic function  $\mathbf{xH}^+$ . Now, the larger electron-donating effect of the **R** substituent diminishes the acidity of this hydrogen, and leads to weaker hydrogen bond (imine series).

Table 3. Proton affinities of the fragments as calculated at the PMP3/aug-cc-pvdz level [kcal mol<sup>-1</sup>].<sup>[a,b]</sup>

Systems	<b>R</b>		
	H <sup>[c]</sup>	CH <sub>3</sub>	NH <sub>2</sub>
PA(1)	178.1	191.8	208.1
PA(2)	187.2	196.9	209.7
PA(3)	216.2	224.2	234.4

[a] As calculated at the same level the proton affinity of  $\cdot\text{NH}_2$  accounts for 193.2 kcal mol<sup>-1</sup>. [b] **1** stands for the carbonyls, **2** for thiocarbonyls, and **3** for imines. [c] From ref. [8].

Table 4. Hydrogen bonded species and corresponding fragments energies.<sup>[a]</sup> The  $\Delta\text{PA}$  values are calculated by use of Equation (1), the  $\mathbf{x} + \text{NH}_3^+$  starting materials being the energy reference. The hydrogen bond strength (italic) are calculated using the lowest dissociative fragments of the bond.

Species	<b>R</b>		
	H <sup>[b]</sup>	CH <sub>3</sub>	NH <sub>2</sub>
<b>1</b> + NH <sub>3</sub> <sup>+</sup>	0.0	0.0	0.0
<b>1H</b> <sup>+</sup> + NH <sub>2</sub>	( $\Delta\text{PA}$ )	15.1	1.4
<b>1HB</b> ( <sup>+</sup> ) <sup>[c]</sup>	( $D_0$ )	23.9	28.7
<b>2</b> + NH <sub>3</sub> <sup>+</sup>	0.0	0.0	0.0
<b>2H</b> <sup>+</sup> + NH <sub>2</sub>	( $\Delta\text{PA}$ )	6.0	-3.7
<b>2HB</b> ( <sup>+</sup> ) <sup>[c]</sup>	( $D_0$ )	18.0	17.9
<b>3</b> + NH <sub>3</sub> <sup>+</sup>	0.0	0.0	0.0
<b>3H</b> <sup>+</sup> + NH <sub>2</sub>	( $\Delta\text{PA}$ )	-23.0	-31.0
<b>3HB'</b>	( $D_0$ )	21.1	19.0

[a] In kcal mol<sup>-1</sup>, PMP3/aug-cc-pvdz/MP2/6–31G(d) level of calculation. [b] From ref. [8]. [c] **HB**- or **HB'**-like hydrogen bond, see Figure 5.

Unfortunately, this acid/base analysis does not allow for a systematic discussion of the hydrogen bond strength, especially when the nature of the hydrogen bond changes within a series (e.g., for carbonyl systems, in which the **HB**-like bond becomes an **HB'**-like one on going from **R** = CH<sub>3</sub> to **R** = NH<sub>2</sub>).

However, the binding-energy modification can be discussed in a more straightforward way by using the  $\Delta\text{PA}$  of the reaction partners. Several parametrized formulas have been published previously. Up to now, they mainly agree on the fact that the bond energy is linearly correlated to the difference in the proton affinities.

Meot-Ner proposed<sup>[21]</sup> that the variation of the hydrogen bond strength in an heteronuclear cationic systems  $\text{AH}^+\text{B}$  ( $D_{\text{AH}^+\text{B}}$ ) follows Equation (5), where  $a$  and  $b$  are fitted parameters; these are given in Table 5 for the different cases of our study.

$$D_{\text{AH}^+\text{B}} = a - b |\Delta\text{PA}| \quad (5)$$

Table 5. Meot-Ner<sup>[21]</sup> parameters relevant for our study.<sup>[a]</sup>

Bond	$a$	$b$
$\text{-NH}^+ \cdots \text{O}$	28.3	0.23
$\text{-NH}^+ \cdots \text{S}$	22.3	0.26
$\text{-NH}^+ \cdots \text{N}$	23.2	0.25

[a] These parameters were optimized for saturated systems.

Larson and McMahon<sup>[22]</sup> suggested another linear dependency of the binding energy on  $\Delta\text{PA}$  in unsymmetrical hydrogen bonded cationic dimers [Eq. (6)].

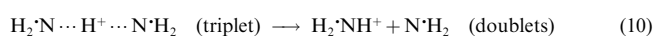
$$D_{\text{AH}^+\text{B}} = D_{\text{AH}^+\text{A}} - 0.5 |\Delta\text{PA}| \quad (6)$$

This second equation is a little more general than Equation (5) in the sense that the  $a$  parameter of Equation (5) is replaced in Equation (6) by the binding energy of one of the symmetrical system  $D_{\text{AH}^+\text{A}}$ , which can be calculated. However, both are empirically optimized formulas and are expected to fail in unexpected cases. Moreover, they do not possess a clear physical meaning.

Marcus theory<sup>[23]</sup> gives a common basis to Equations (5) and (6) as we will see in the following. When applied to two parabolas with negative curvatures (inverted barrier),<sup>[24]</sup> Marcus theory leads to Equation (7), in which  $D$ , as indicated in Equation (8), is the average of the dissociation energies of the symmetrical proton bonded dimers  $D_{\text{AH}^+\text{A}}$  and  $D_{\text{BH}^+\text{B}}$ . The values of  $D_{\text{AH}^+\text{A}}$  and  $D_{\text{BH}^+\text{B}}$  can be calculated by using the dissociation reactions given in Equations (9) and (10), respectively.

$$D_{\text{AH}^+\text{B}} = D - |\Delta\text{PA}|/2 + |\Delta\text{PA}|^2/16D \quad (7)$$

$$D = (D_{\text{AH}^+\text{A}} + D_{\text{BH}^+\text{B}})/2 \quad (8)$$



It is noteworthy that Equation (7) resembles Equation (5), if the  $a$  parameter is read as  $D$ , and if one considers the  $b$

parameter ( $b \approx 1/4$ ) to be and approximation of  $1/2 - |\Delta PA| / 16D$ . Equation (7) resembles also Equation (6) in a similar manner.

Another way of describing the hydrogen binding in cationic species is to consider its resonating nature as suggested when the barrier of the proton transfer is small or non-existent.<sup>[10, 11, 18, 24, 25]</sup> This resonating nature possesses similarities with the three electron bond. When adapted from the  $2c-3e$  bond to our hydrogen bond problem, Equation (2) leads to Equation (11).<sup>[26]</sup> It is interesting to note that when  $\Delta PA$  is small before  $2D$ , Equation (11) can be expanded into a Taylor series and leads to Equation (12), which resembles the Marcus Equation (7).<sup>[27]</sup>

$$D_{\text{AH}^+\text{B}} = -(|\Delta PA| - \sqrt{|\Delta PA|^2 + (2D)^2})/2 \quad (11)$$

$$D_{\text{AH}^+\text{B}} = D - |\Delta PA|/2 + |\Delta PA|^2/8D \quad (12)$$

We also note that only the last term differs in the Marcus Equation (7). For small  $\Delta PA$ , both descriptions are equivalent. However, the Equations (11) and (12) are derived from the resonating nature of the bond. Therefore, it will be in the following of special interest to compare the different descriptions, and show what part the resonance plays in the binding energy.

The MP2/6-31G(d) optimized geometries<sup>[28]</sup> of the symmetrical proton-bonded dimers  $\text{AH}^+\text{A}$  and  $\text{BH}^+\text{B}$  are displayed in Figure 7. For the sake of simplicity we calculated the

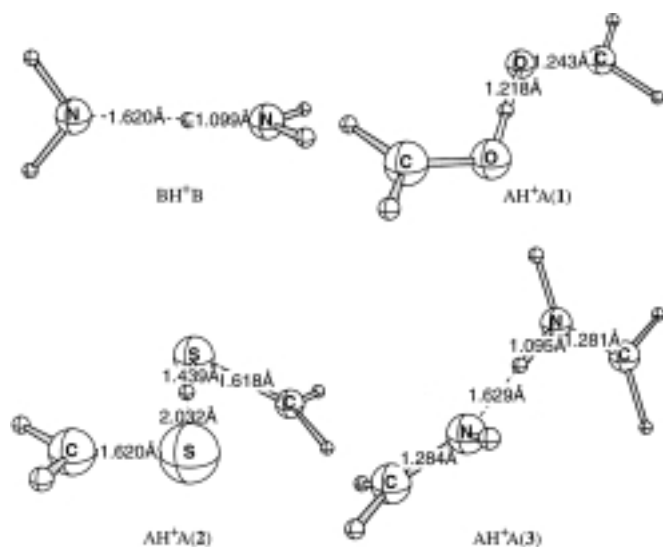


Figure 7. Homonuclear hydrogen bonded species.  $\text{BH}^+\text{B}$  is the biradical triplet, which most resembles the proton-bonded dimer of the  $\cdot\text{NH}_2$  moiety. The  $\text{AH}^+\text{A}$  systems are closed shell singlets. Following the previous notation we name them  $\text{AH}^+\text{A}(1)$  for the carbonyl,  $\text{AH}^+\text{A}(2)$  thionyl, and  $\text{AH}^+\text{A}(3)$  imine cases.

values of  $D$  [Eqs. (7)–(11)] only for the unsubstituted cases ( $\mathbf{R} = \text{H}$ ), and used them for all the cases ( $\mathbf{R} = \text{H}, \text{CH}_3, \text{NH}_2$ ). The binding energy  $D_{\text{AH}^+\text{A}}$  is indeed not expected to vary much in such symmetrical systems.<sup>[24]</sup>

The numerical results of Equation (11) as well as the values of  $D_{\text{AH}^+\text{A}}$ ,  $D_{\text{BH}^+\text{B}}$  are shown in Table 6. In order to present an

Table 6. Hydrogen bond strength<sup>[a]</sup> as estimated by using various approximations, compared with the calculated values  $D_0$  and  $\Delta PA$ .<sup>[a]</sup>

Species	H	R		
		CH <sub>3</sub>	NH <sub>2</sub>	
<b>1HB</b> (*) <sup>[c]</sup>	( $\Delta PA$ )	15.1	1.4	-14.9
	Eq. (5) <sup>[c]</sup>	24.8	28.0	24.9
	Eq. (6) <sup>[d]</sup>	23.2	30.0	23.3
	Eq. (7)	21.3	27.7	21.4
	Eq. (11)	21.8	27.7	21.9
$D_{\text{AH}^+\text{A}}(\mathbf{1}) = 30.7$	( $D_0$ ) <sup>[a]</sup>	<b>23.9</b> <sup>[b]</sup>	<b>28.7</b>	<b>25.6</b>
<b>2HB</b> (*) <sup>[c]</sup>	( $\Delta PA$ )	6.0	-3.7	-16.5
	Eq. (5) <sup>[c]</sup>	21.3	20.7	18.0
	Eq. (6) <sup>[d]</sup>	23.0	24.2	17.8
	Eq. (7)	18.2	19.2	13.6
	Eq. (11)	18.3	19.3	14.4
$D_{\text{AH}^+\text{A}}(\mathbf{2}) = 16.1$	( $D_0$ ) <sup>[a]</sup>	<b>18.0</b> <sup>[b]</sup>	<b>17.9</b>	<b>15.3</b>
<b>3HB</b> '	( $\Delta PA$ )	-23.0	-31.0	-41.2
	Eq. (5) <sup>[c]</sup>	17.5	15.5	12.9
	Eq. (6) <sup>[d]</sup>	15.9	11.9	6.8
	Eq. (7)	16.4	13.4	10.1
$D_{\text{AH}^+\text{A}}(\mathbf{3}) = 27.4$	Eq. (11)	17.6	15.4	13.1
	( $D_0$ ) <sup>[a]</sup>	<b>21.1</b> <sup>[b]</sup>	<b>19.0</b>	<b>16.8</b>

[a] In  $\text{kcal mol}^{-1}$  from PMP3/aug-cc-pvdz//MP2/6-31G(d) level of calculation.  $D_{\text{BH}^+\text{B}} = 26.0 \text{ kcal mol}^{-1}$  at this level. [b] From ref. [8]. [c] By using Equation (5) and the appropriate parameters from Table 5. [d] By using Equation (6) with the largest of  $D_{\text{AH}^+\text{A}}$  and  $D_{\text{BH}^+\text{B}}$  for  $D_{\text{AH}^+\text{A}}$ . [e] **HB**- or **HB'**-like hydrogen bond, see Figure 5.

homogeneous treatment, we also included the results obtained when using Equations (5), (6) and (7).

Equation (11) agrees reasonably well with the fully calculated values ( $D_0$ ). In some cases, an underestimation of about  $3-4 \text{ kcal mol}^{-1}$  on the binding energy is obtained. On the other hand, the empirical linear Equations (5) and (6) do not perform much better. Equation (6) was optimized only for oxygen atoms, and it is not surprising that it fails for the other cases. Equation (5), however, uses a specific set of parameters for each kind of system, and also displays a small error (about  $\pm 3-4 \text{ kcal mol}^{-1}$ ) when compared with the fully calculated values.

The small underestimation of the binding energy by using Equation (11) is found to be correlated with  $\Delta PA$ . It is particularly manifest for imine cases. As  $\Delta PA$  gets large, the resonance gets low and Equation (11) underestimates the binding energy, indicating that as the resonance diminishes, another interaction (electrostatic for instance) increases. As this modification is not taken into account in our equation, we expect the underestimation of the binding energy to be more important for larger  $\Delta PA$ . A correction could be done by adding an electrostatic term of minor contribution, for instance: Most of the electrostatic interactions are already taken into account by using  $(D_{\text{AH}^+\text{A}} + D_{\text{BH}^+\text{B}})/2$  in Equation (11). The error might thus correspond to a modification of this term when the proton gets more strongly bonded to the X atom as in the imine cases (large  $\Delta PA$ ). This correction is, however, not trivial, and should be tested on a large variety of examples, which is beyond the interest of this paper.

The results of both the Marcus theory [Eq. (7)] and Equation (11), based on the resonance model, are shown in Figure 8 for the imine cases. As mentioned earlier, both descriptions are similar, especially when  $\Delta PA$  is small.

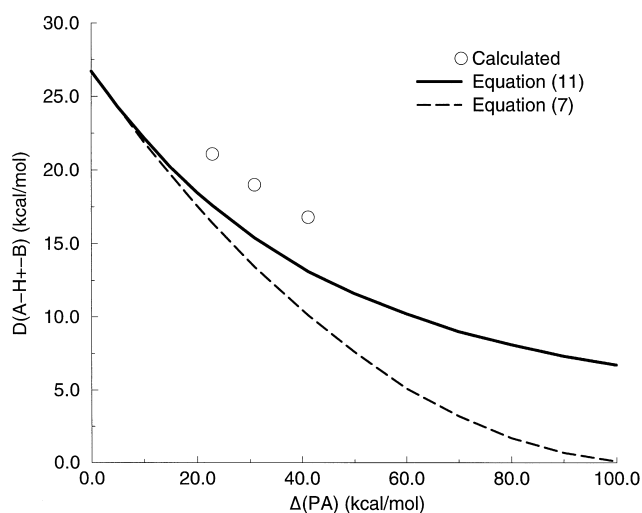


Figure 8. Hydrogen bond energy as a function of  $\Delta PA$  for large  $\Delta PA$  in the case of the imines. The calculated points (circles) are the results from the MP3/aug-cc-pvdz//MP2/6–31G(d) level.

## Conclusion

We have determined the substituents effects on the bond strengths of the 2c–3e bonds between a variety of unsaturated organic functional groups and the ammonia radical cation ( $\text{NH}_3^{+\cdot}$ ). Using the valence bond theory, we related the 2c–3e bond strength variation to the IPs of fragments. In the case of endothermic SET ( $\Delta IP > 0$ ,  $\mathbf{X} = \text{O}$ ), electron-donating substituents increase the strength of the 2c–3e bond, while in the case of exothermic SET, these substituents diminish the bond strength.

We also calculated the corresponding hydrogen bonded complexes which compete with the 2c–3e interaction. In both cases, bond energies were found to be in the same range of 20–30 kcal mol<sup>-1</sup>. The resonating model of 2c–3e bonds can be applied to the description of the hydrogen binding in those cationic systems. Equation (11) accounts for most of the binding energy, even for quite large  $\Delta PA$ . More data are, however, required to confirm this finding. Nevertheless, we have also shown that Marcus theory and the resonance model of the hydrogen bond are very similar, especially in the case of low  $\Delta PA$ .

## Acknowledgement

A substantial computing time allocation of institute “IDRIS”, project 98 10 46, is gratefully acknowledged.

- [1] a) P. M. Gill, L. Radom, *J. Am. Chem. Soc.* **1998**, *110*, 4931; b) T. Clark, *J. Am. Chem. Soc.* **1988**, *110*, 1672.  
 [2] a) Y. Wang, *Chem. Phys. Lett.* **1985**, *116*, 286; b) W. Hub, S. Schneider, F. Dörr, J. D. Oxman, F. D. Lewis, *J. Am. Chem. Soc.* **1984**, *106*, 701.  
 [3] See for instance: a) L. S. Nichols, M. L. McKee, A. J. Illies, *J. Am. Chem. Soc.* **1998**, *120*, 1538; b) S. P. de Visser, L. J. de Konning, N. M. M. Nibbering, *J. Am. Chem. Soc.* **1998**, *120*, 1517; c) K.-D. Asmus, *Acc. Chem. Res.* **1979**, *12*, 436; d) K.-D. Asmus, D. Bahne-mann, Ch.-H. Fischer, D. Veltwish, *J. Am. Chem. Soc.* **1979**, *101*, 5322; e) Y. Deng, A. J. Illies, M. A. James, M. L. McKee M. Peschke, *J. Am.*

*Chem. Soc.* **1995**, *117*, 420; f) J. C. Scaiano, S. Garcia, H. Garcia, *Tetrahedron Lett.* **1997**, *38*, 5929; g) R. W. Alder, *Acc. Chem. Res.* **1983**, *16*, 321; h) W. Wang, M. N. Schuchmann, H.-P. Schuchmann, W. Knolle, J. von Sonntag, C. von Sonntag, *J. Am. Chem. Soc.* **1999**, *121*, 238.

- [4] a) S. Humbel, P. C. Hiberty, I. Demachy, *Chem. Phys. Lett.* **1995**, *247*, 126; b) P. C. Hiberty, S. Humbel, S. Shaik, D. Danovitch, *J. Am. Chem. Soc.* **1995**, *117*, 9003.  
 [5] N. C. Baird, *J. Chem. Educ.* **1977**, *54* 291.  
 [6] P. C. Hiberty, S. Humbel, P. Archirel, *J. Phys. Chem.* **1994**, *98*, 11 697.  
 [7] For cationic systems see: a) M. Bonifacis, I. Stefanic, G. L. Hug, D. A. Armstrong, K.-D. Asmus, *J. Am. Chem. Soc.* **1998**, *120*, 9930; b) K. Bobrowsky, G. L. Hug, B. Marciniak, B. Miller, C. Schöneich, *J. Am. Chem. Soc.* **1997**, *119*, 8000; c) M. A. James, M. L. McKee, A. J. Illies, *J. Am. Chem. Soc.* **1996**, *118*, 7836; for neutral systems see: d) M. L. McKee, A. Nicolaidis, L. Radom, *J. Am. Chem. Soc.* **1996**, *118*, 10571.  
 [8] S. Humbel, I. Côte, N. Hoffmann, J. Bouquant, *J. Am. Chem. Soc.* **1999**, *121*, 5507.  
 [9] The 2c–3e complex must involve the radical and the lone pair of the organic substrate. An interaction with the  $\pi$  system is not favorable, since such an interaction would partly depopulate a bonding orbital (low in energy).  
 [10] There is a subtle difference between these terms. See, for example, Y. Pan, M. A. McAllister, *J. Am. Chem. Soc.* **1998**, *120*, 166.  
 [11] a) S. Scheiner, T. Kar, *J. Am. Chem. Soc.* **1995**, *117*, 6970; b) S. Scheiner, *J. Am. Chem. Soc.* **1981**, *103*, 315.  
 [12] J. Fossey, personal communication (1999).  
 [13] M. J. Frisch, G. W. Trucks, H. B. Schlegel, P. M. W. Gill, B. G. Johnson, M. A. Robb, J. R. Cheeseman, T. Keith, G. A. Petersson, J. A. Montgomery, K. Raghavachari, M. A. Al-Laham, V. G. Zakrzewski, J. V. Ortiz, J. B. Foresman, J. Cioslowski, B. B. Stefanov, A. Nanayakkara, M. Challacombe, C. Y. Peng, P. Y. Ayala, W. Chen, M. W. Wong, J. L. Andres, E. S. Replogle, R. Gomperts, R. L. Martin, D. J. Fox, J. S. Binkley, D. J. Defrees, J. Baker, J. P. Stewart, M. Head-Gordon, C. Gonzalez, J. A. Pople, *Gaussian 94, Revision E.2*, Gaussian, Pittsburgh PA, **1995**.  
 [14] D. E. Woon, T. H. Dunning, Jr., *J. Chem. Phys.* **1993**, *90*, 1358.  
 [15] Five d orbitals were used with this aug-cc-pvdz basis set (5D).  
 [16] a) S. Humbel, S. Sieber, K. Morokuma, *J. Chem. Phys.* **1996**, *105*, 1959; b) S. Dapprich, I. Komaromi, K. S. Byun, K. Morokuma, *J. Mol. Struct. (THEOCHEM)* **1999**, *461–462*, 1.  
 [17] When comparing PMP3/6–31G(d,p)//MP2/6–31G(d) and the IMO-MO-ONIOM: CCSD(T):MP2/6–31G(d,p)//MP2/6–31G(d) levels. See S. Humbel, *J. Mol. Struct. (THEOCHEM)* **1999**, *461–462*, 153.  
 [18] See, for example, a) S. Scheiner, L. Wang, *J. Am. Chem. Soc.* **1993**, *115*, 1958; b) E. Uggerud, *J. Am. Chem. Soc.* **1996**, *116*, 6873.  
 [19] Optimized at the MP2/6–31G(d) level in the  $C_s$  symmetry, three of these structures have one low imaginary frequency (Transition State): ( $\mathbf{R} = \text{CH}_3$ ) **1TE**, **1HB**, and ( $\mathbf{R} = \text{NH}_2$ ) **3TE**. Their reoptimizations were therefore carried out without symmetry. However, we found that the unsymmetrical ( $C_1$ ) structures were slightly higher in energy than the corresponding  $C_s$  structures. The potential energy surface is extremely flat vis-à-vis the corresponding coordinates. We kept only the most symmetrical one for the high-level calculations.  
 [20] As a binding energy has to be calculated using the lowest dissociative fragments, the binding energy in the formamidine case, for example, is 42.5 – 21.8 = 20.7 kcal mol<sup>-1</sup>.  
 [21] M. Meot-Ner, *J. Am. Chem. Soc.* **1984**, *106*, 1257.  
 [22] J. W. Larson, T. B. McMahon, *J. Am. Chem. Soc.* **1982**, *106*, 6255.  
 [23] a) R. A. Marcus, *J. Phys. Chem.* **1968**, *72*, 891; b) A. J. Kresge, *Acc. Chem. Res.* **1975**, *354*; c) O. Cohen, R. A. Marcus *J. Phys. Chem.* **1968**, *72*, 4249.  
 [24] a) S. Scheiner, P. Redfern, *J. Phys. Chem.* **1986**, *90*, 2969; b) D. E. Magnoli, J. R. Murdoch, *J. Am. Chem. Soc.* **1981**, *103*, 7465, and references therein.  
 [25] Similar behavior can be found in anionic species, see, for example, M. Garcia-Viloca, A. Gonzalez-Lafont, J. M. Lluch, *J. Am. Chem. Soc.* **1997**, *119*, 1081.  
 [26] When  $\Delta IP$  is replaced by  $\Delta PA$ , and  $D_{AA}$ ,  $D_{BB}$  by  $D_{AH+A}$ ,  $D_{BH+B}$  respectively.  
 [27] The same kind of expansion was done in ref. [6] and lead to the exponential variation of the 2c–3e binding energy as shown in



Equation (3). Similarly, our proposal could be formulated to show an exponential variation of the proton binding energy toward  $\Delta PA$  for small  $\Delta PA$ . Such an expression could be compared with the empirical expression proposed by T. Zeegers-Huyskens, *J. Mol. Struct.* **1988**, *177*, 125:  $D_{AH^+B} = x \exp(-x' |\Delta PA|)$ . One would therefore find  $x \approx D$  and  $x' \approx 1/(2\sqrt{D_{AH^+A} D_{BH^+B}})$ .

[28] It is found that the geometry optimization of the  $AH^+A$  systems collapsed to unsymmetrical hydrogen bonded complexes in all cases

but the carbonyl one (which bear a symmetrical minimum). In all the other cases the symmetrical structure was found to be a transition state to the proton transfer, and we preferred to use the unsymmetrical  $D_{AH^+A}$  in these cases.

Received: July 1, 1999 [F1885]